JOURNAL OF MATERIALS SCIENCE 13 (1978) 2676–2686

A study of the homogenization process of aluminium-zinc alloys

R. CIACH, B. DUKIET-ZAWADZKA
Institute for Metal Research, Polish Academy of Sciences, Reymonta 25, 30-059 Kraków, Poland
T. D. CIACH
University of Mining and Metallurgy, Mickiewicza 30, 30-059 Kraków, Poland

This paper is concerned with theoretical and experimental studies of the dendritic structure and its dissolution in aluminium–zinc alloys. The maximal dendritic micro-segregation in the composition range of the α solid solution, as defined by the amount of non-equilibrium $\alpha + \eta$ eutectic, and the variation in zinc concentration across a model of dendritic grain have been calculated. The measurements of the above mentioned quantities were then performed using quantitative microscopy and X-ray microanalysis. The results obtained for the as-cast Al–Zn alloys confirmed the theoretically predicted data. In order to eliminate such micro-segregation an annealing treatment was applied. Specimens of Al 60 wt% Zn alloy (0.383 mole fraction of zinc) showed a significant resistance to the homogenization treatment. This phenomenon can be explained theoretically on the basis of the calculated homogenization relaxation time, and the thermodynamical factor $d\mu_{Zn}/dN_{Zn}$, for several annealed alloys. Both of these quantities achieve their maximum in the composition range 0.30 to 0.40 mole fraction of zinc.

Nomenclature

K	crystallization coefficient
N^x_{Zn}	the mole fraction of zinc in the liquid at a given stage of crystallization
$N^x_{(Zn)}$	the mole fraction of zinc in the solid formed on the dendrite surface at a given stage of crystallization
n^0_{Zn}	amount of zinc in one mole of alloy
$n^0_{(Zn)}$	amount of zince in a dendrite at a given stage of crystallization
x	amount of dendritic constituent in one mole of solidified alloy
c	constant calculated for the boundary value $x = 0$ and for the mole fraction of zinc in the initial liquid of the examined alloy
$\bar{N}^x_{(Zn)}$	a mean content of zinc (in a mole fraction) at any arbitrary stage of solidification
N^0_{Zn}	the total amount of zinc in the alloy (in a mole fraction)
D^*_{Zn}, D^*_{Al}	the self-diffusion coefficients for zinc and aluminium
$\tilde{D}$	the interdiffusion coefficient
N_{Zn}, N_{Al}	the mole fraction of aluminium and zinc in alloy
f	the thermodynamic factor equal to $1 + (d \ln \gamma_{Zn}/d \ln N_{Zn})$
γ_{Zn}	the activity coefficient of zinc
τ	the relaxation time of the homogenization process
l	the radius of the dendrite cell
J_{Zn}	flux of zinc diffusion in the solid solution
μ_{Zn}	the chemical potential of zinc
M	the phenomenological coefficient of diffusion
x_1	the thickness of the considered diffusion layer

1. Introduction

Aluminium–zinc alloys, according to the equilibrium diagram in the range of composition 0 to 66.5 at% Zn, are expected to solidify as a single phase solid solution. However, the structures of the as-cast alloys usually reveal, besides the

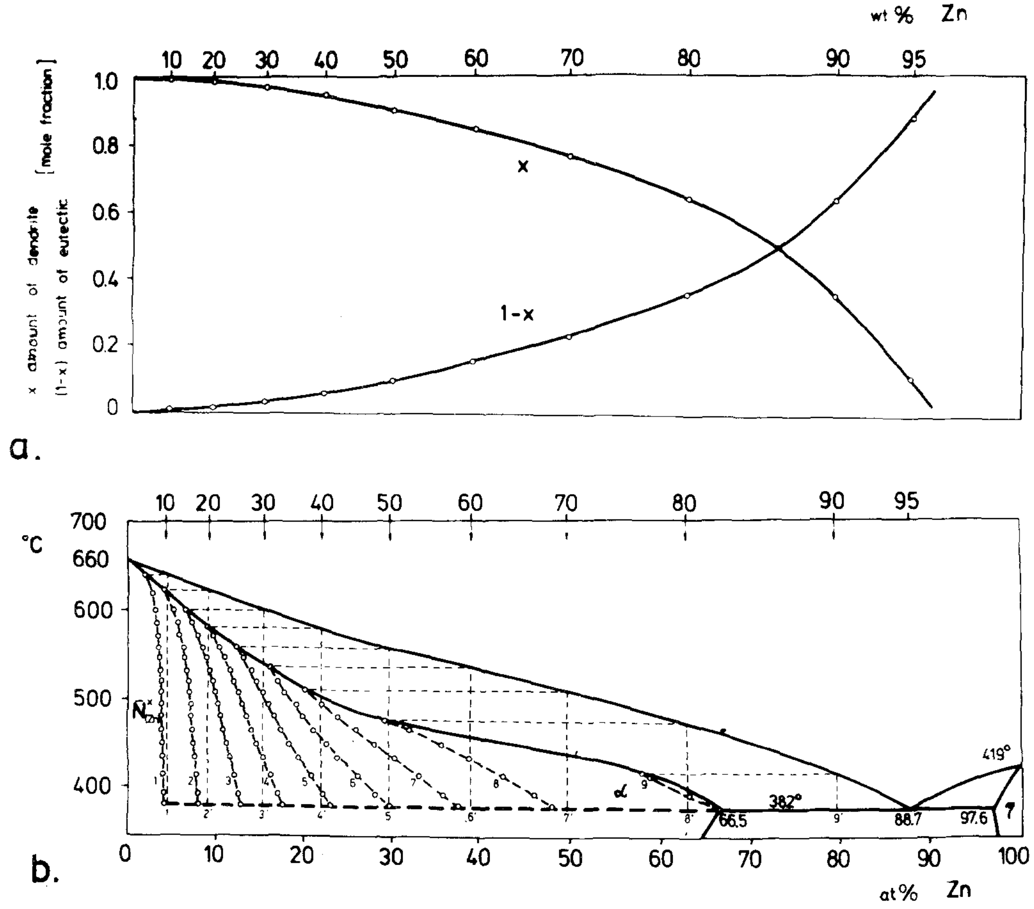

Figure 1 (a) Theoretically calculated amount of non-equilibrium ($\alpha + \eta$) eutectic ($1 - x$) existing in aluminium–zinc alloys in assumed condition of solidification; (b) modified solidus lines in the aluminium–zinc phase diagram for assumed condition of solidification.

unequal distribution of zinc within the dendritic grains, also sometimes the presence of a non-equilibrium eutectic. This lack of homogeneity in the composition range of the α phase is one of the important reasons for the observed instability of mechanical and several physical properties. As was shown in a previous paper [1], the rate of decomposition of the supercooled α phase increases significantly with increasing Zn content in this phase. Therefore, in order to stabilize the properties of aluminium–zinc alloys, special attention must be paid to the degree of micro-segregation in the as-cast alloys, and to its proper elimination during homogenization by annealing.

2. Theoretical and experimental procedure

The theoretical and experimental study of the homogenization process was done on cast alloys containing 40 to 70 wt% of zinc, of similar grain size, approximately 50 μm in diameter.

The theoretical maximal dendritic micro-segregation was defined using Krupkowski's method [2], which assumes complete diffusion in the liquid, no diffusion in the solid, and takes into account the changes in the distribution coefficient, K, during solidification. Equation 1 presents Krupkowski's solution and was derived from the basic defintion of the distribution coefficient. After some rearrangement and solving Equation 2, the final Equation 5 was obtained as follows:

$$K = \frac{N^x_{(\mathrm{Zn})}}{N^x_{\mathrm{Zn}}} = \frac{1 - x}{n^0_{\mathrm{Zn}} - n^x_{(\mathrm{Zn})}} \cdot \frac{\mathrm{d}n^x_{(\mathrm{Zn})}}{\mathrm{d}x} \tag{1}$$

$$\frac{1}{1 - K}\,\mathrm{d}\ln N^x_{\mathrm{Zn}} = -\mathrm{d}\ln(1 - x) \tag{2}$$

$$\frac{1}{1 - K} = f(-\ln N^x_{\mathrm{Zn}}) \tag{3}$$

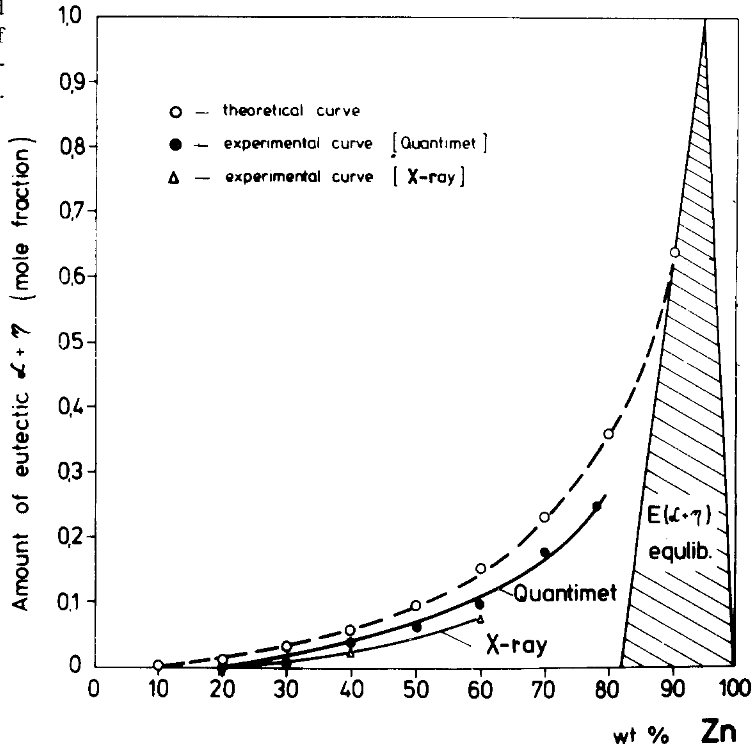

Figure 2 Theoretically calculated and experimentally measured amount of non-equilibrium ($\alpha + \eta$) eutectic existing in aluminium–zinc cast alloys.

$$\frac{1}{1-K} = 1.12 - 0.217 \ln N^{x}_{\mathrm{Zn}} - \frac{0.368}{\ln N^{x}_{\mathrm{Zn}}} \quad (4)$$

$$-1.12 \ln N^{x}_{\mathrm{Zn}} + 0.1085 \ln (N^{x}_{\mathrm{Zn}})^2 + 0.368 \ln (\ln N^{x}_{\mathrm{Zn}}) = \ln(1-x) + c \quad (5)$$

The assumed values of zinc content in the liqud phase, and the calculated amounts of dendritic constituent x in the same consecutive stage of crystallization enable us to calculate the average zinc content at a dendrite using the formula:

$$\bar{N}^{x}_{(\mathrm{Zn})} = \frac{N^{0}_{\mathrm{Zn}} - N^{x}_{\mathrm{Zn}}(1-x)}{x} \quad (6)$$

From this result the theoretical non-equilibrium solidus line can be plotted as in Fig. 1b. On the upper part of this diagram the non-equilibrium amount of the eutectic $(1-x)$, as well as the amount of solidified dendrites x, are presented. Note the increase in the amount of the eutectic with the increase of zinc content.

Fig. 2 shows the comparison of the calculated data and the experimental results obtained using the quantitative microscope "Quantimet" and an X-ray diffractometer. These results demonstrate the significant dendritic non-homogeneity of the examined alloys [3, 5].

The calculated changes in the chemical composition were referred to a cubic model [9] of the dendritic solidification of one mole of the alloy. The cross-section of the model for the Al–60 wt% Zn alloy, shown in Fig. 3b, gives the maximum changes in the solute concentration within the assumed cubic model. In the centre of the microcell a wide region of low concentration of zinc exists and on approaching the cell boundary the concentration rapidly increases. The non-equilibrium ($\alpha + \eta$) eutectic and the cored structure of the α solid solution in the Al–40 wt% Zn, Al–60 25% Zn and Al–70 wt% Zn alloys are shown in Fig. 4. Changes of zinc concentration within the grains were determined using an X-ray microanalyser. The composite figures showing the microprobe traces across dendrites are given in Figs. 5a, b and c. They are similar to the results predicted theoretically in Fig. 3b.

Several metallographic examinations revealed strong persistence of the dendritic structure of Al–60 wt% Zn alloy (0.383 Zn mole fraction), homogenized in the temperature range close to 360° C. Figs. 6 and 7 show the structures of examined alloys before and after annealing; the former obtained with an optical microscope and the latter using the scanning electron microscope.

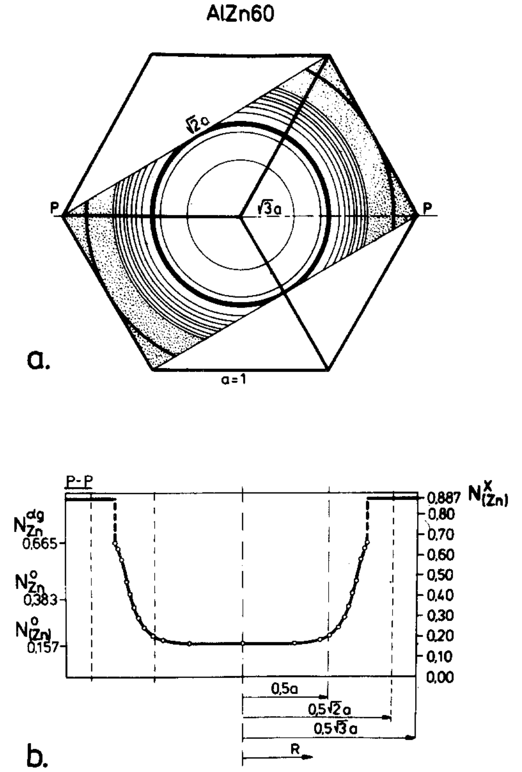

Figure 3 (a) Spherical model of a dendrite cell of Al–60 wt% Zn alloy; (b) theoretically calculated curve of the change in zinc concentration in a dendrite microcell of Al–60 wt% Zn alloy.

The residual dendritic structure of the Al–60 wt% Zn alloy after 50 h homogenization at 360° C is visible in Fig. 7b. This observation was confirmed by the results obtained by scan-line microprobe analysis (Fig. 8) which show changes of chemical composition in dendritic cells of different as-cast alloys. The effect of annealing is shown in Fig. 9, in which the difference in zinc content is marked only for the Al–60 wt% Zn alloy.

To explain this phenomenon the changes of interdiffusion coefficient $\tilde{D}$ versus the zinc content in the alloy was calculated according to the Darken equation [4, 7]:

$$\tilde{D} = [D^*_{Zn} \cdot N_{Al} + D^*_{Al} \cdot N_{Zn}] \cdot f \qquad (7)$$

The self-diffusion coefficient of zinc D^*_{Zn}, was taken from the paper by Hilliard *et al.* [6]. According to this work, the self-diffusion of aluminium is much lower than for zinc in the aluminium–zinc alloys and thus can be ignored. Fig. 10 shows the changes of self-diffusion coefficient D^* versus zinc content for several temperatures. The thermodynamic factor $f = 1 + (\mathrm{d}\ln\gamma_{Zn}/\mathrm{d}\ln N_{Zn})$ was defined using Krupkowski's equation [8, 9] for the activity coefficient γ_{Zn}. The changes of the thermodynamic factor f with zinc content are shown in Fig. 11.

From these two different behaviours of f and D^* results the typical character of the calculated changes of the interdiffusion coefficient $\tilde{D}$ versus

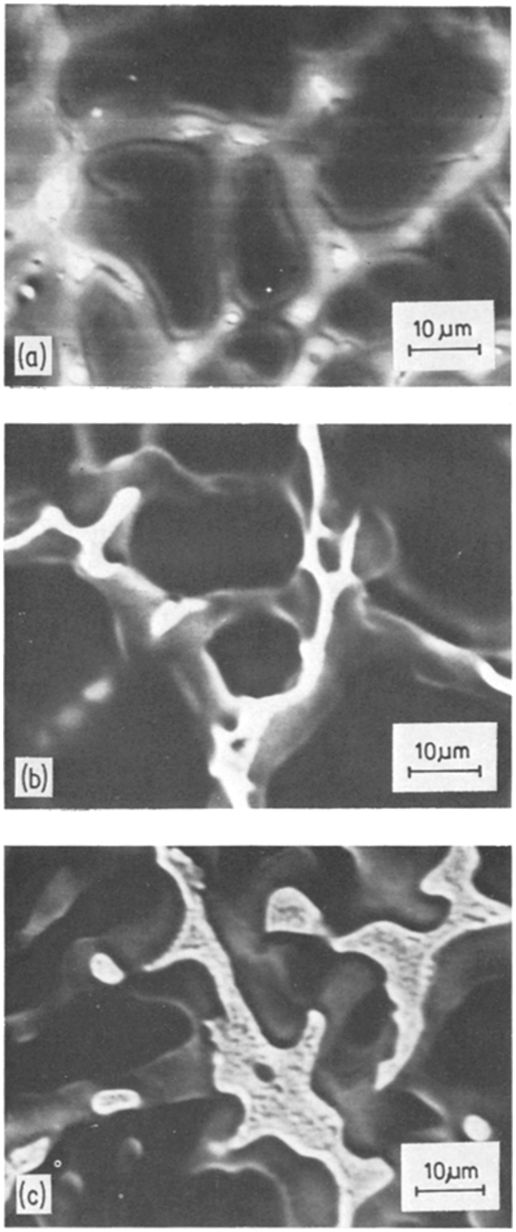

Figure 4 Scanning electron micrographs taken from (a) Al–40 wt% Zn; (b) Al–60 wt% Zn; (c) Al–70 wt% Zn alloys.

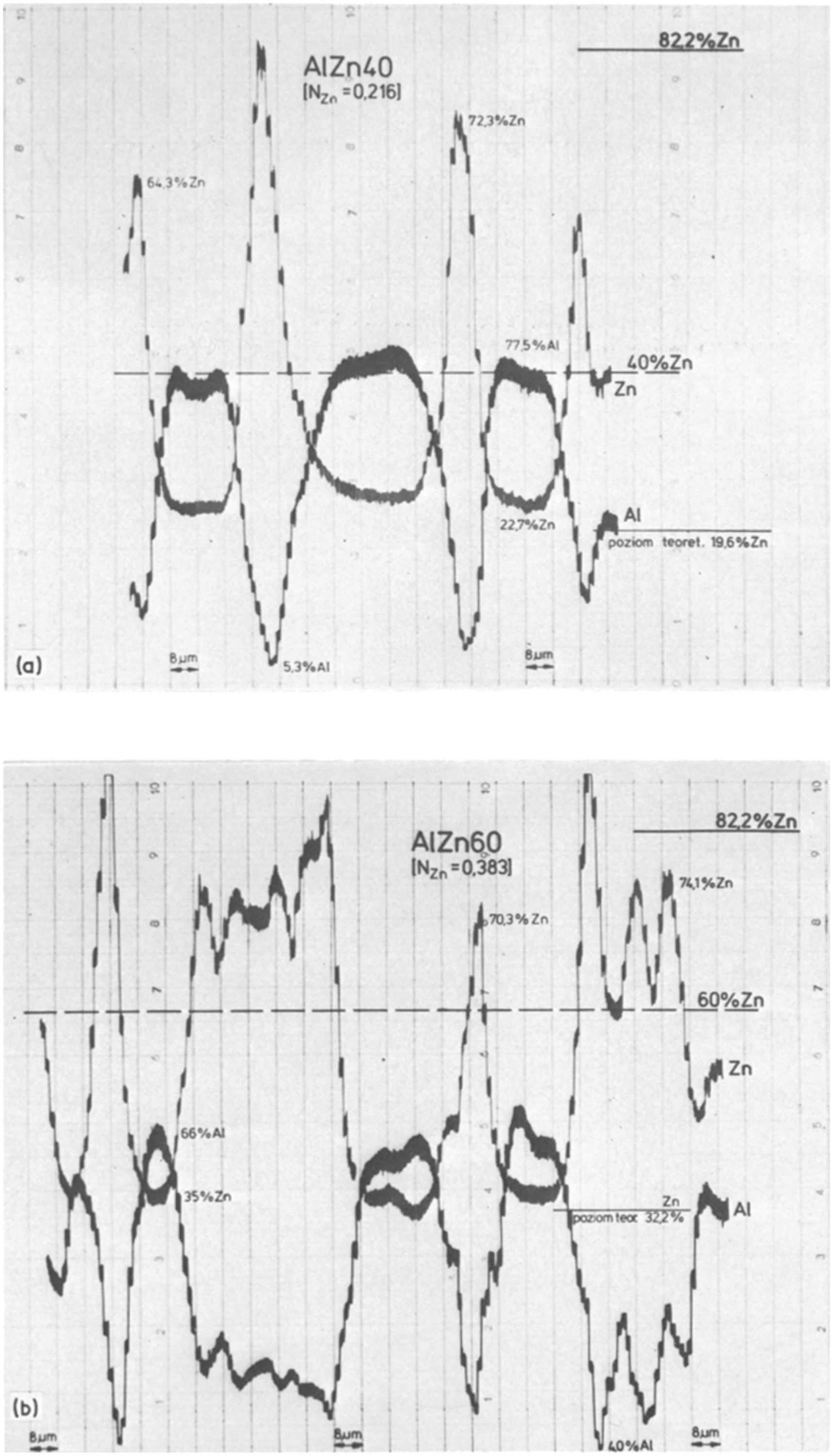

Figure 5 The change in zinc and aluminium concentration in the dendritic structure of (a) Al–40 wt% Zn alloy; (b) Al–60 wt% Zn alloy; (c) Al–70 wt% Zn alloy, measured using an X-ray microanalyser.

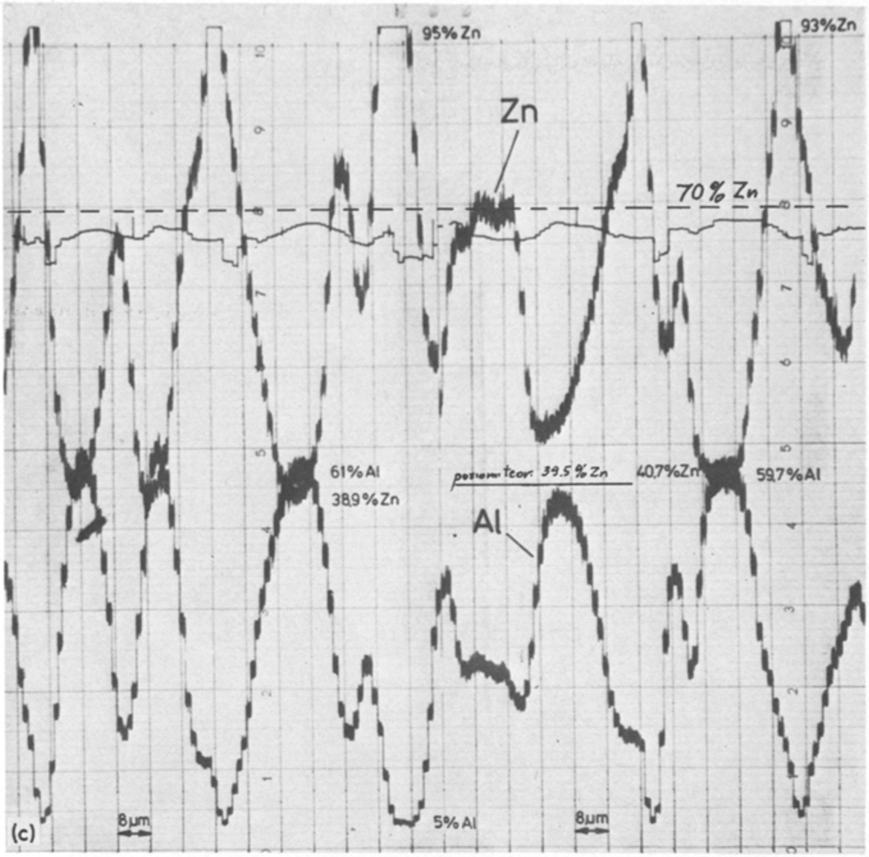

Figure 5 continued

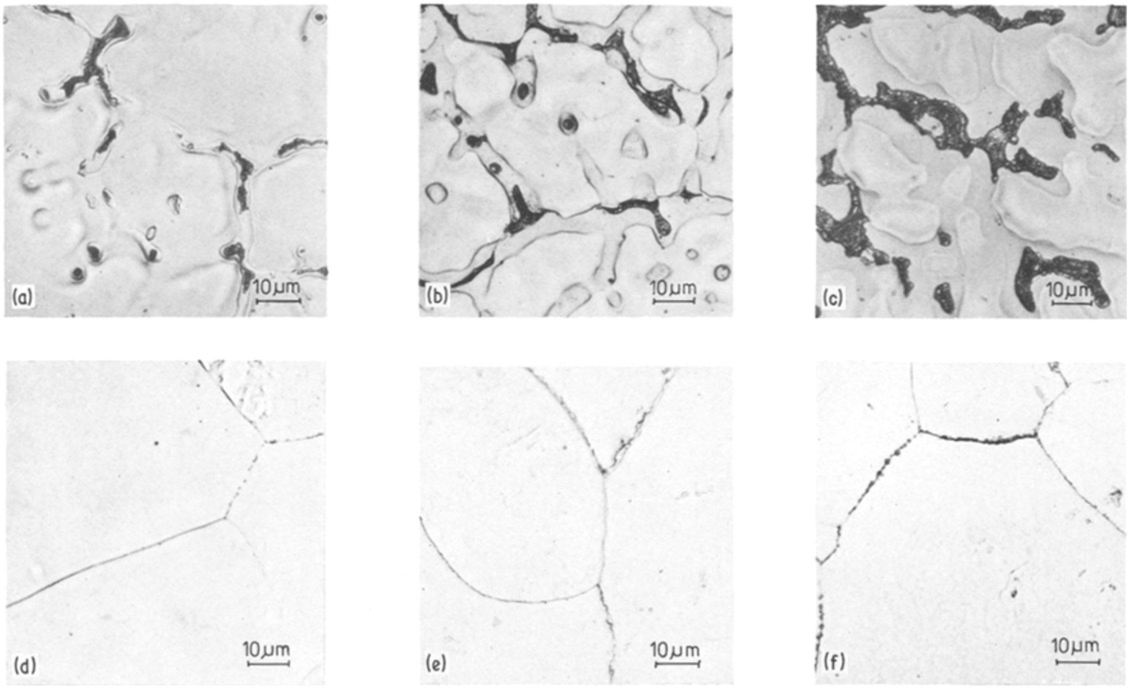

Figure 6 Micrographs of the cast (a) Al–40 wt% Zn; (b) Al–60 wt% Zn; (c) Al–70 wt% Zn alloys. (d–f) Structures after annealing at 360° C for 50 h.

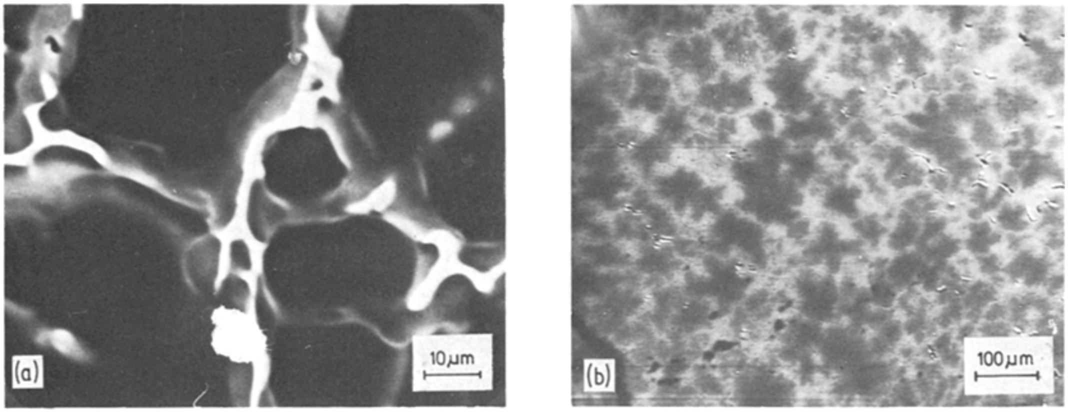

Figure 7 Scanning electron micrographs (a) of the cast Al–60 wt% Zn alloy; (b) after homogenization annealing at 360° C for 50 h.

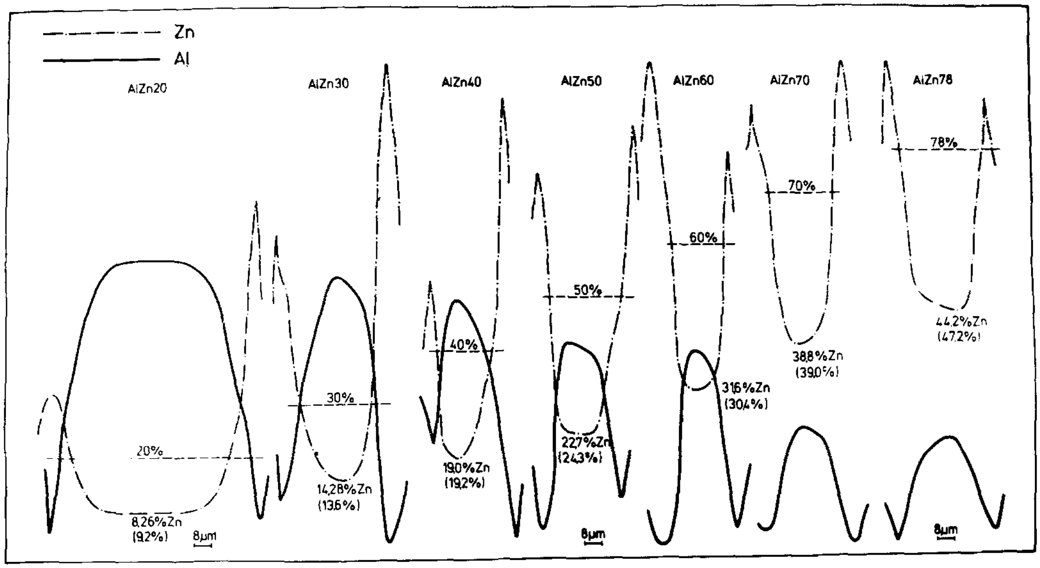

Figure 8 The change of zinc and aluminium concentration in dendrites of Al–20, 30, 40, 50, 60, 70 and 78 wt% Zn alloys, obtained using an X-ray microanalyser.

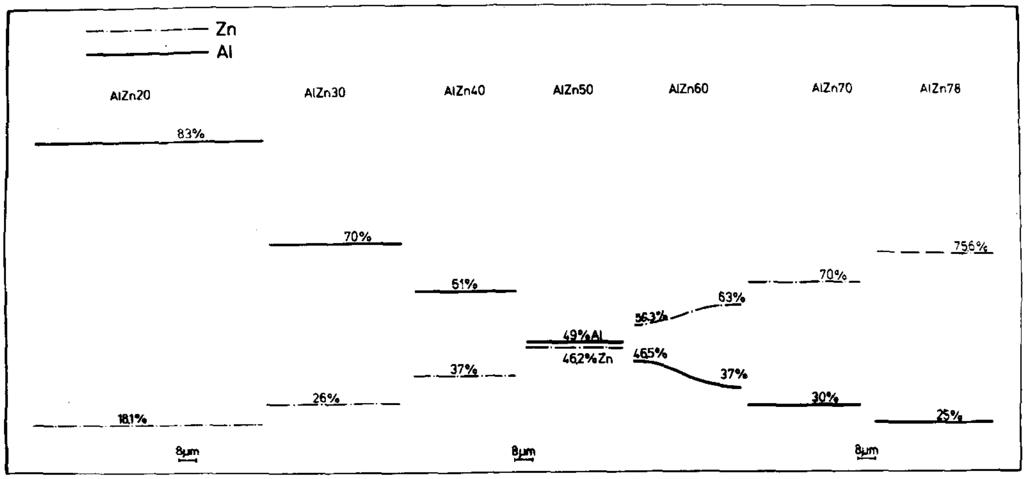

Figure 9 The change of zinc and aluminium concentration in grains of Al–20, 30, 40, 50, 60, 70 and 78 wt% Zn alloys after homogenization annealing at 360° C for 50 h.

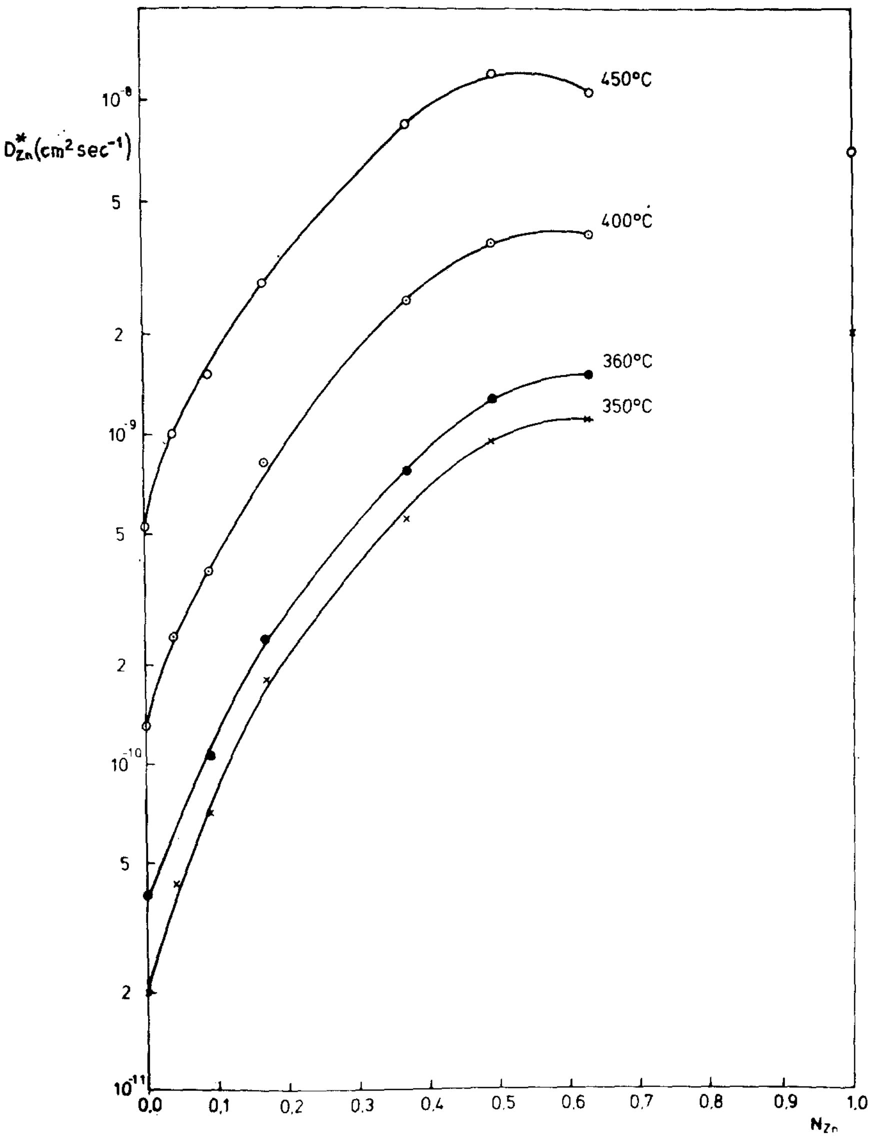

Figure 10 Changes in the self-diffusion coefficient D^* with zinc content in aluminium–zinc alloys and temperatures used in the homogenization process.

zinc content in the aluminium–zinc alloys, as shown in Fig. 12. According to this diagram the interdiffusion coefficient decreases rapidly when the zinc content increases from 0.0 to 0.3 mole fraction, and within the range 0.31 to 0.40 it approaches its minimum value. As shown in this diagram, this tendency is smaller at the higher temperature.

The effects of the above changes of the interdiffusion coefficient are more evident when the relaxation time of the homogenization process is plotted against the zinc content, as shown in Fig. 13. The relaxation time is calculated on the basis of Shewmon's theory of homogenization [4] using the following equation:

$$\tau = \frac{l^2}{\pi^2 \tilde{D}} \qquad (8)$$

On the other hand the velocity of the diffusion is proportional to the gradient of the chemical potential, $\mathrm{d}\mu_{Zn}/\mathrm{d}x_1$ according to the Darken phenomenological formula for the flux of diffusion:

$$J_{Zn} = M\frac{\mathrm{d}\mu_{Zn}}{\mathrm{d}x}, \qquad (9)$$

where

$$M = \frac{-D_{Zn}c_{Zn}}{RT}.$$

The chemical potential of zinc versus the zinc content in the alloy at several temperatures was

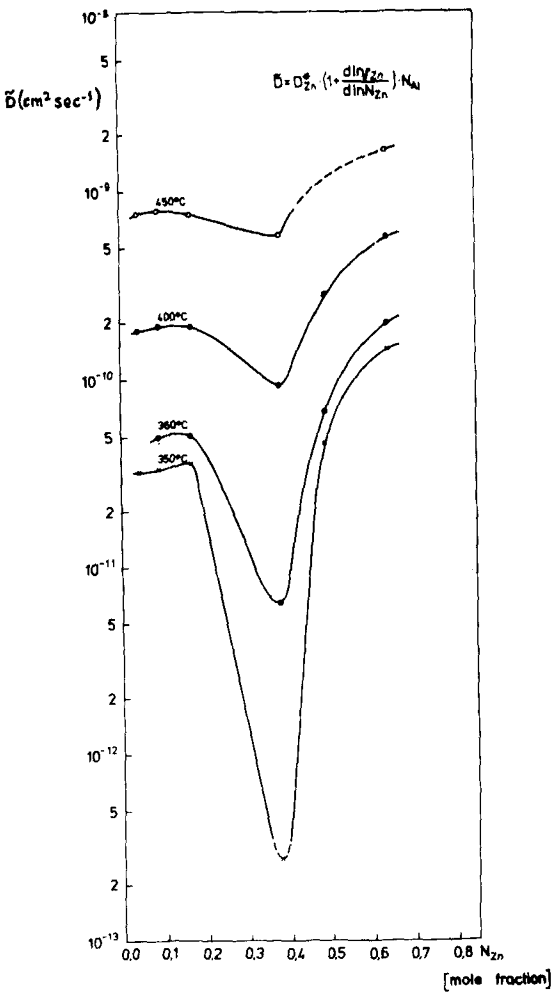

Figure 11 Changes in the thermodynamic factor $f = 1 + (d\ln\gamma_{Zn}/d\ln N_{Zn})$ with zinc content and temperature in aluminium–zinc alloys.

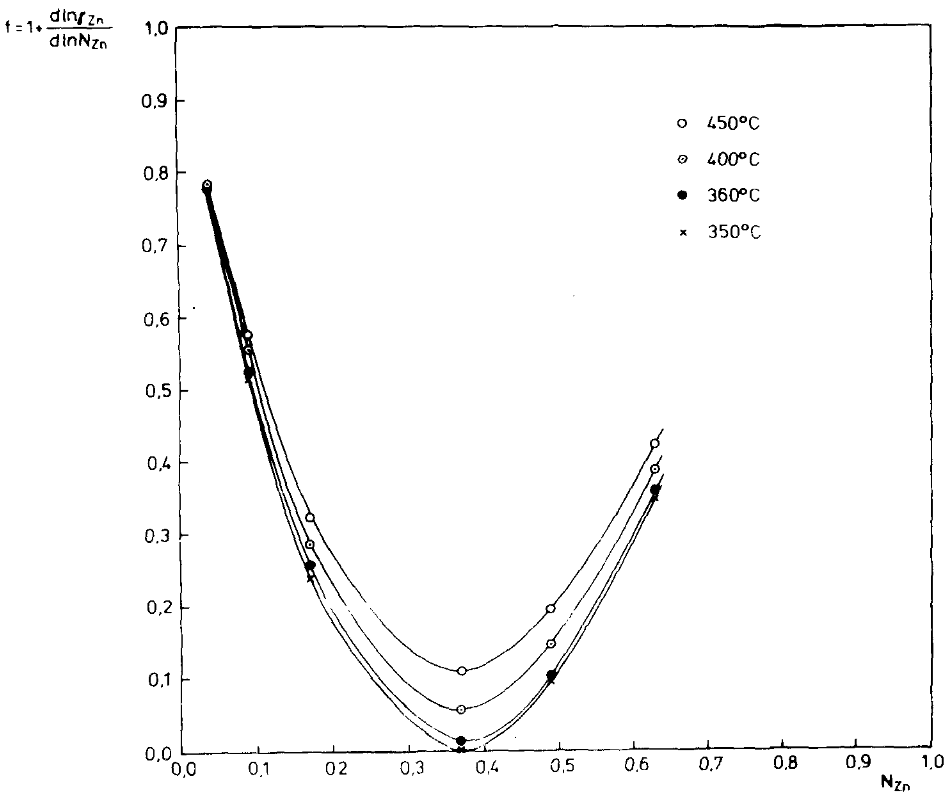

Figure 12 Changes in the interdiffusion coefficient $\tilde{D}$ with zinc content in aluminium–zinc alloys.

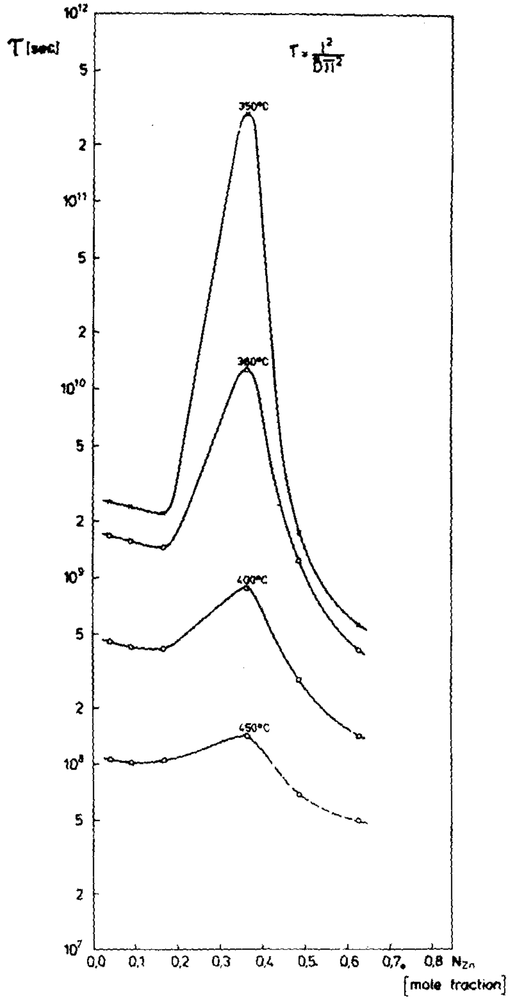

Figure 13 Changes in the relaxation time with zinc content and annealing temperature in aluminium–zinc alloys.

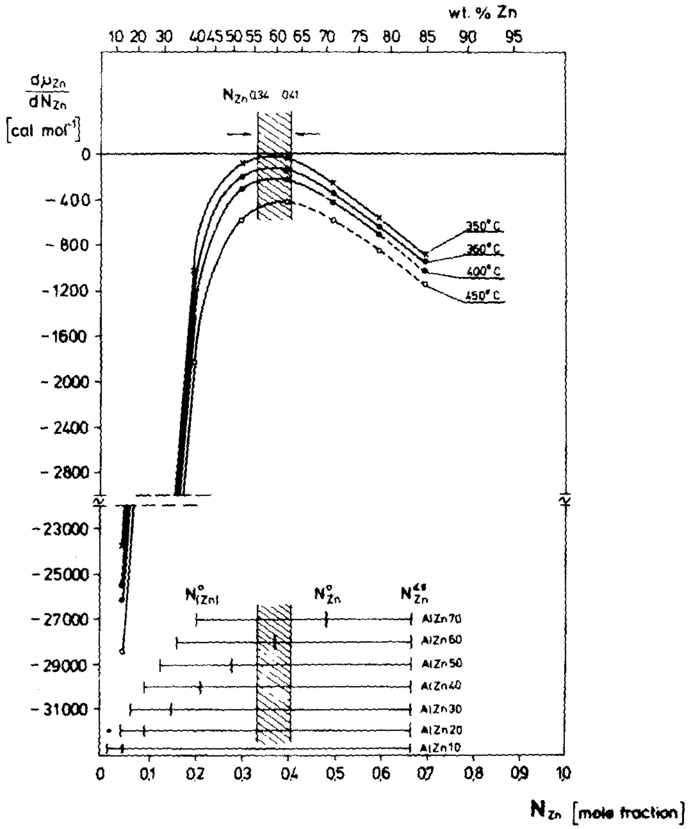

Figure 14 Changes in the thermodynamic factor $d\mu_{Zn}/dN_{Zn}$ with zinc content and temperature in aluminium–zinc alloys.

calculated using the corresponding values of the free energy of α solid solution (the data were taken from the paper by Ciach [8] regarding the transformation energy of the h c p zinc to a corresponding hypothetical f c c structure). The diagram in Fig. 14 shows that the thermodynamic factor $d\mu_{Zn}/dN_{Zn}$ approaches 0 in the range 0.31 to 0.42 mole fraction of zinc in the alloy. The full agreement between theory and experiments explains the delay of the homogenization processes in the Al–60 wt% Zn alloy.

3. Conclusion

A significant micro-segregation of zinc was observed in aluminium–zinc cast alloys, and is described theoretically. A comparison between the experimentally measured amount of non-equilibrium $(\alpha + \eta)$ eutectic with that calculated according to Krupkowski's theory shows a very good agreement.

A persistent stability of the dendritic structure of the Al–60 wt% Zn alloy was observed during the annealing treatment. A theoretical calculation of some diffusion and thermodynamic factors of the investigated alloys revealed the following: a minimum in the interdiffusion coefficient $\tilde{D}$; a maximum in the relaxation time τ of the homogenization process, and the thermodynamic factor $d\mu_{Zn}/dN_{Zn}$ approaching zero in the alloys in the composition range 55 to 60 wt% zinc. These results explain the slow rate of diffusion in the Al–60 wt% Zn cast alloy, which ought therefore to be homogenized for a much longer time than other aluminium–zinc alloys.

To eliminate dendritic micro-segregation in aluminium–zinc cast alloys, a two stage heat treatment process is suggested. Annealing at the temperature 360° C would cause dissolution of the non-equilibrium $(\alpha + \eta)$ eutectic, while a second stage would homogenize the α solid solution at a higher temperature.

References

1. A. KRUPKOWSKI, R. CIACH and J. KRÓL, *Bull. Acad. Pol. Sci., Ser. Sci. Technol.* **11** (1967) 25.
2. A. KRUPKOWSKI, *ibid.* **10** (1968) 1.
3. B. DUKIET-ZAWADZKA and R. CIACH, Proceedings of the IX Conference PAN-STOP Kraków (1976) **1**, 96.
4. P. G. SHEWMON, "Diffusion in Solids" (McGraw-Hill, New York, 1963).
5. B. DUKIET-ZAWADZKA, Dissertation, ZPM PAN, Kraków, unpublished (1976).
6. J. E. HILLIARD, B. L. AVERBACK and M. COHEN, *Acta Met.* 9 (1959) 86.
7. K. FITZNER and K. WIENCEK, *Bull. Acad. Pol. Sci. Ser. Sci. Technol.* **12** (1975) 31.
8. R. CIACH, *Arch. Hutn.* **19** (1974) 27.
9. A. KRUPKOWSKI, *ibid.* **12** (1967) 343.

Received 14 March and accepted 20 March 1978.